SPATIALLY-SMOOTH PIECE-WISE CONVEX ENDMEMBER DETECTION

Alina Zare†, Ouiem Bchir, Hichem Frigui*, and Paul Gader†*

†Department of Computer and Information Science and Engineering, University of Florida
*Computer Engineering and Computer Science Department, University of Louisville

ABSTRACT

An endmember detection and spectral unmixing algorithm that uses both spatial and spectral information is presented. This method, Spatial Piece-wise Convex Multiple Model Endmember Detection (Spatial P-COMMEND), autonomously estimates multiple sets of endmembers and performs spectral unmixing for input hyperspectral data. Spatial P-COMMEND does not restrict the estimated endmembers to define a single convex region during spectral unmixing. Instead, a piece-wise convex representation is used that can effectively represent non-convex hyperspectral data. Spatial P-COMMEND drives neighboring pixels to be unmixed by the same set of endmembers encouraging spatially-smooth unmixing results.

Index Terms— Hyperspectral, Endmember, Spectral Unmixing, Convex Geometry Model, Linear Mixing Model, Fuzzy C-Means, Spatial.

1. INTRODUCTION

During hyperspectral endmember detection and spectral unmixing, the frequently used convex geometry model states that each pixel in a hyperspectral image can be described with a convex combination of the endmembers [1].

$$\mathbf{x}_i = \sum_{k=1}^{M} p_{ik}\mathbf{e}_k + \epsilon_i \quad i = 1, \ldots, N \tag{1}$$

where N is the number of pixels, M is the number of endmembers, ϵ_i is an error term, p_{ik} is the abundance of endmember k in pixel i, and $\mathbf{e}_k$ is the k^{th} endmember. The abundances of this model satisfy the constraints in Equation 2,

$$p_{ik} \geq 0 \quad \forall k = 1, \ldots, M; \quad \sum_{k=1}^{M} p_{ik} = 1. \tag{2}$$

When the convex geometry model is applied globally over an input image with a single set of endmembers, the input hyperspectral image is represented as a single convex region. However, hyperspectral images are often not convex such as the AVIRIS Indian Pines data set shown in Figure 1 [2]. As shown in Figures 1(b) and 1(c), the Indian Pines data is not convex. The P-COMMEND [3] and the Spatial P-COMMEND algorithms represent hyperspectral imagery using several sets of endmembers that allows for accurate representation of non-convex hyperspectral images. Given a set of endmembers, each pixel in the input image can be unmixed following the convex geometry model in Equation 1. The piece-wise convex representation for hyperspectral imagery was first developed in [4] and [5]. Endmember detection methods that incorporate spatial information include [7, 8, 9]. However, these methods do not employ a piece-wise convex model.

In the following, Section 2 outlines the P-COMMEND algorithm, Section 3 introduces the spatial extension of P-COMMEND, Section 4 presents experimental results and Section 5 provides a discussion and conclusions.

2. P-COMMEND

The P-COMMEND algorithm [3] performs alternating optimization to autonomously estimate the endmembers, $\mathbf{E}$, abundances, $\mathbf{P}$, and membership values, $\mathbf{U}$, for a given hyperspectral image. P-COMMEND iteratively minimizes the objective function in Equation 3 subject to the constraints in Equation 2, $\sum_{i=1}^{C} u_{ij} = 1$ and $u_{ij} \geq 0$.

$$\begin{aligned} J &= \sum_{i=1}^{C}\sum_{j=1}^{N} u_{ij}^{m} \left(\mathbf{x}_j - \mathbf{p}_{ij}\mathbf{E}_i\right)\left(\mathbf{x}_j - \mathbf{p}_{ij}\mathbf{E}_i\right)^T \\ &+ \alpha \sum_{i=1}^{C} \left(M \cdot trace(\mathbf{E}_i\mathbf{E}_i^T) - 1_{1\times M}\mathbf{E}_i\mathbf{E}_i^T 1_{M\times 1}\right) \end{aligned} \tag{3}$$

where $\mathbf{x}_j$ is a $1 \times d$ vector representing the j^{th} pixel of the image, N is the number of pixels in the image, M is the number of endmembers in each convex region (or model), P_i is a $N \times M$ matrix such that $\mathbf{p}_{ij}$, is the vector of abundances associated with pixel j with respect to model i, p_{ijk} is the proportion of endmember k in pixel j with respect to model i, and $\mathbf{E}_i$ is a $M \times d$ matrix such that each row of $\mathbf{E}_i$, $\mathbf{e}_{ik}$, is

Research was supported by NSF program Optimized Multi-algorithm Systems for Detecting Explosive Objects Using Robust Clustering and Choquet Integration (CBET-0730484). The views and conclusions contained in this document are those of the authors and should not be interpreted as representing the official policies, either expressed or implied, of NSF. The U. S. Government is authorized to reproduce and distribute reprints for Government purposes notwithstanding any copyright notation hereon.

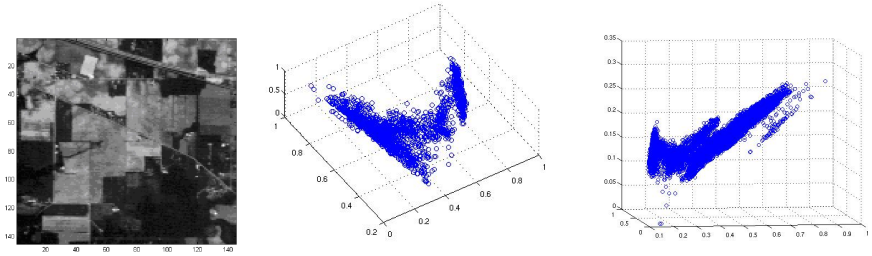

(a) (b) (c)

Fig. 1. (a) Band 10 (0.49 μm) of the AVIRIS Indian Pines data set The Indian Pines data set after dimensionality reduction to three dimensions using (b) PCA and (c) Hierarchical Dimensionality reduction [6].

a $1 \times d$ vector representing the k^{th} endmember with respect to model i. The notation $1_{S\times T}$ denotes an $S \times T$ matrix with all entries equal to 1. The multiple models compete for data $\mathbf{X}$ through a set of weights u_{ij} which represent the memberships of the data points $\mathbf{X}$ in the i^{th} model where m is the "fuzzifier" parameter controlling the degree to which the data points are shared among the models.

The first term of this objective function computes the residual error incurred by representing each spectra using the estimated endmembers, abundances and fuzzy membership values. The use of the fuzzy membership values is related to the fuzzy c-means algorithm and the Multiple Model General Linear Regression [10, 11]. The second term is related to the volume enclosed by the endmembers by computing the sum of squared distances (SSD) between the endmembers and encourages the endmembers to have a tight fit around the data. The SSD term is the same volume-related term used by ICE and SPICE for endmember detection [12, 13].

When updating membership values, the objective function is minimized subject to the constraint that all the membership values for a data point must sum to one. This results in the following update equation given abundances and endmembers,

$$u_{ij} = \frac{1}{\sum_{q=1}^{C} \left(\frac{(\mathbf{x}_j - \mathbf{p}_{ij}\mathbf{E}_i)(\mathbf{x}_j - \mathbf{p}_{ij}\mathbf{E}_i)^T}{(\mathbf{x}_j - \mathbf{p}_{qj}\mathbf{E}_q)(\mathbf{x}_j - \mathbf{p}_{qj}\mathbf{E}_q)^T} \right)^{\frac{1}{m-1}}}. \quad (4)$$

The endmembers are updated given the following equation,

$$\mathbf{E}_i = \left(\sum_j u_{ij}^m \mathbf{p}_{ij}^T \mathbf{p}_{ij} + 2\alpha D \right)^{-1} \left(\sum_j u_{ij}^m \mathbf{p}_{ij}^T \mathbf{x}_j \right) \quad (5)$$

where $D = MI_{M\times M} - 1_{M\times M}$. Finally, abundance values are updated by minimizing Equation 3 subject to the constraints in Equation 2 by using a Lagrange multiplier term to enforce the sum-to-one constraints and evaluating and applying the required KKT conditions for the non-negativity constraints. The resulting update equations are

$$\mathbf{p}_{ij}^T = \left(\mathbf{E}_i \mathbf{E}_i^T\right)^{-1} \left(\mathbf{E}_i \mathbf{x}_j^T - \frac{\lambda_{ij}}{2} 1_{M\times 1} \right) \quad (6)$$

and

$$\mathbf{p}_{ij}^{KKT} = max\left(\mathbf{p}_{ij}^T, 0\right) \quad (7)$$

where $\lambda_{ij} = 2\frac{1_{1\times M}\left(\mathbf{E}_i\mathbf{E}_i^T\right)^{-1}\mathbf{E}_i\mathbf{x}_j^T - 1}{1_{1\times M}\left(\mathbf{E}_i\mathbf{E}_i^T\right)^{-1}1_{M\times 1}}$.

3. SPATIAL P-COMMEND

The Spatial P-COMMEND algorithm extends P-COMMEND by incorporating spatial information to aid in estimating endmembers and abundance values. Spatial information is incorporated by encouraging neighboring pixels in the image to have similar membership values to the different convex regions. This is accomplished in Spatial P-COMMEND by adopting the spatially-smooth fuzzy c-means method, FLICM, developed in [14]. The FLICM algorithm adds a "fuzzy factor" term, G, to the objective function that influences the updates of the membership values by incorporating spatial information. The G term, adapted for use in the Spatial P-COMMEND algorithm, is shown in Equation 8.

$$G_{ij} = \sum_{\substack{k\in N_j \\ j\neq k}} \frac{1}{d_{jk}+1} (1-u_{ij})^m \, ||\mathbf{x}_j - \mathbf{p}_{ij}\mathbf{E}_i||_2^2 \quad (8)$$

where the $\mathbf{x}_j$ is the center pixel in the local window under consideration, N_j is the neighborhood around the center pixel (such as a 3x3 window), d_{ij} is the Euclidean distance between the image indices between $\mathbf{x}_j$ and $\mathbf{x}_k$. Therefore, the G term scales the influence of neighboring pixels based on their distance in the index space. Also, when a neighboring pixel has high membership in a convex region, the point under consideration is encouraged to also have a high membership in that region. The fuzzy factor term is updated each iteration and treated as a constant during updates to the endmembers, abundances and membership values. With the addition of G, the objective function for Spatial P-COMMEND is shown in

Equation 9.

$$J = \sum_{i=1}^{C}\sum_{j=1}^{N} u_{ij}^{m}\left(\left(\mathbf{x}_j - \mathbf{p}_{ij}\mathbf{E}_i\right)\left(\mathbf{x}_j - \mathbf{p}_{ij}\mathbf{E}_i\right)^T + G_{ij}\right) + \alpha\sum_{i=1}^{C}\left(M \cdot trace(\mathbf{E}_i\mathbf{E}_i^T) - 1_{1\times M}\mathbf{E}_i\mathbf{E}_i^T 1_{M\times 1}\right) \quad (9)$$

In Spatial P-COMMEND, the update equations for the endmembers and abundances remain the same as in Equations 5 and 7. Membership updates change as shown in Equation 10.

$$u_{ij} = \frac{1}{\sum_{q=1}^{C}\left(\frac{(\mathbf{x}_j-\mathbf{p}_{ij}\mathbf{E}_i)(\mathbf{x}_j-\mathbf{p}_{ij}\mathbf{E}_i)^T+G_{ij}}{(\mathbf{x}_j-\mathbf{p}_{qj}\mathbf{E}_q)(\mathbf{x}_j-\mathbf{p}_{qj}\mathbf{E}_q)^T+G_{qj}}\right)^{\frac{1}{m-1}}}. \quad (10)$$

The Spatial P-COMMEND algorithm performs alternative optimization on the endmembers, abundances and memberships until some stopping criterion is reached such as convergence or a maximum number of iterations.

4. EXPERIMENTAL RESULTS

The Spatial P-COMMEND algorithm was applied to simulated two-dimensional data. The simulated image was 100x20 pixels in size with the first 50 rows contained spectra that were randomly generated from endmembers at (0,0), (3, 0) and (1.5, 4.5). The second 50 rows contained spectra that were randomly generated from endmembers located at (0,3), (3,3), and (1.5,6). P-COMMEND was also applied to this data. The parameters used for both the Spatial P-COMMEND and P-COMMEND algorithms were $\alpha = 0.01$, $m = 1.5$, $M = 3$, $C = 2$. The results using P-COMMEND are shown in Figure 2. As shown in Figure 2(c), several pixels from the first 50 rows were incorrectly partitioned into the second set of endmembers (the top triangle) and the regions enclosed by the estimated endmembers do not overlap like the regions defined by the true endmembers used to generate the data. However, when incorporating spatial information, the estimated endmembers correctly overlap and are a much better estimate of the true endmembers, as shown in Figure 2(b).

P-COMMEND and Spatial P-COMMEND were also run on the three-dimensional AVIRIS Indian Pines data shown in Figure 1(c). The results found using the two methods are shown in Figure3. When compared to P-COMMEND, Spatial P-COMMEND found more appropriate overlapping convex regions. The parameters used to generate these results were $\alpha = 0.001$, $m = 1.5$, $M = 3$, $C = 3$. As with the simulated data, Spatial P-COMMEND effectively used spatial information to determine endmembers that better match the input hyperspectral data. Consider the Soybeans-min class in this data set. As shown in Figure 3(c), this class is incorrectly partitions this class across all three convex regions estimated by P-COMMEND; in contrast, Spatial P-COMMEND correctly placed the entire class into a single convex region. Similar results with the corn-notill class are also shown in Figure 3.

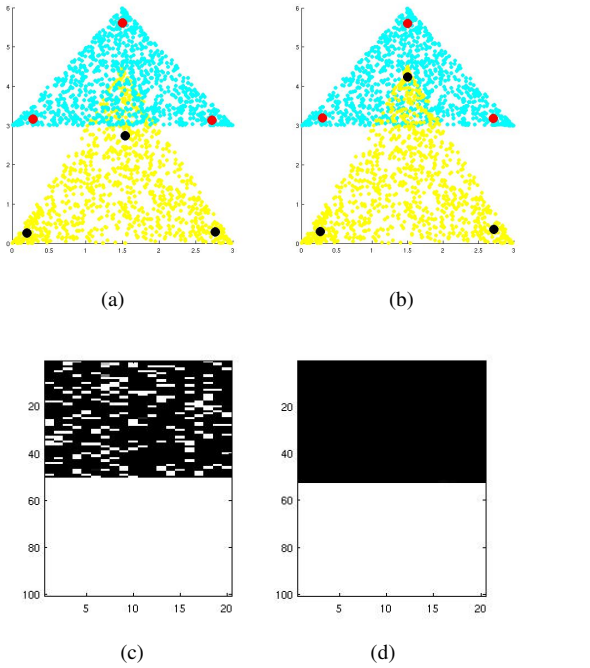

Fig. 2. Scatter plot of simulated data generated from two sets of endmembers and estimated endmember using (a) P-COMMEND. (b) Spatial P-COMMEND. Image of partitioning of data points into the convex regions found by (c) P-COMMEND and (d) Spatial P-COMMEND.

5. DISCUSSION AND CONCLUSIONS

P-COMMEND is able to estimate endmembers and perform spectral unmixing for non-convex hyperspectral data sets. In addition, Spatial P-COMMEND uses spatial information to better estimate the endmembers that represent the data. Future work in enhancing P-COMMEND and Spatial P-COMMEND include autonomously estimating the number of convex regions and the number endmembers in each convex region as well as autonomously setting the α parameter.

6. REFERENCES

[1] N. Keshava and J. F. Mustard, "Spectral unmixing," *IEEE Signal Processing Magazine*, vol. 19, pp. 44–57, 2002.

[2] AVIRIS, "Free standard data products.," (2004, Sep) Jet Propulsion Laboratory, California Institute of Technology, Pasedena, CA. URL http://aviris.jpl.nasa.gov/html/aviris.freedata.html.

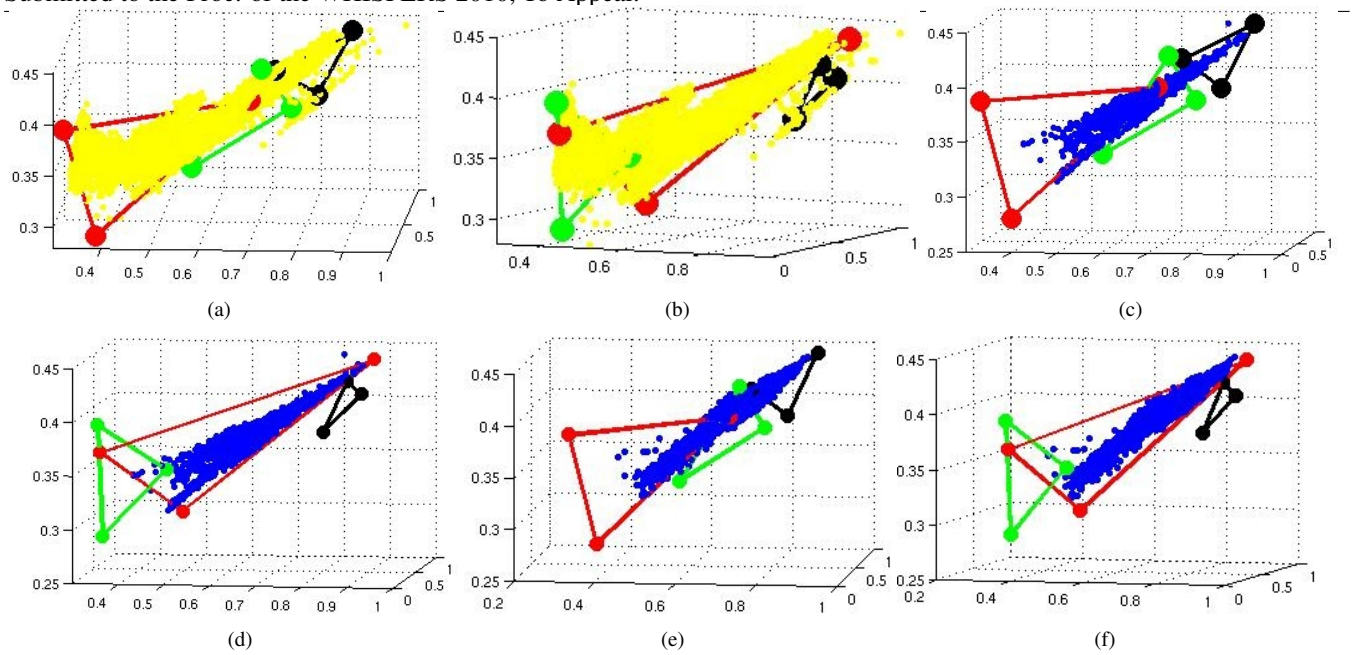

Fig. 3. Scatter plot of AVIRIS Indian Pine data after hierarchical dimensionality reduction to 3 dimensions and endmembers estimated using (a) P-COMMEND. (b) Spatial P-COMMEND. Scatter plot of AVIRIS Indian Pines data from the Soybeans-min class and endmembers estimated using (c) P-COMMEND and (d) Spatial P-COMMEND. Scatter plot of AVIRIS Indian Pines data from the Corn-notill class and endmembers estimated using (e) P-COMMEND and (f) Spatial P-COMMEND.

[3] A. Zare, O. Bchir, H. Frigui, and P. Gader, "Piece-wise convex multiple model endmember detection," *IEEE Trans. on Geoscience and Remote Sensing*, Submitted.

[4] A. Zare, *Hyperspectral Endmember Detection and Band Selection using Bayesian Methods*, Ph.D. thesis, University of Florida, 2009.

[5] A. Zare and P. Gader, "PCE: Piece-wise convex endmember detection," *IEEE Trans. on Geoscience and Remote Sensing*, To Appear.

[6] A. Martinez-Uso, F. Pla, J. M. Sotoca, and P. Garcia-Sevilla, "Clustering-based hyperspectral band selection using information measures," *IEEE Transactions on Geoscience and Remote Sensing*, vol. 45, no. 12, pp. 4158–4171, Dec. 2007.

[7] A. Plaza, P. Martinez, R. Perez, and J. Plazas, "Spatial/spectral endmember extraction by multidimensional morphological operators," *IEEE Trans. on Geoscience and Remote Sensing*, vol. 40, no. 9, pp. 2025–2041, Sept. 2002.

[8] D. M. Rogge, B. Rivard, J. Zhang, A. Sanchez, J. Harris, and J. Feng, "Integration of spatial-spectral information for the improved extraction of endmembers," *Remote Sensing of Environment*, vol. 110, pp. 287–303, 2007.

[9] M. Zortea and A. Plaza, "Spatial preprocessing for endmember extraction," *IEEE Trans. on Geoscience and Remote Sensing*, vol. 47, no. 11, pp. 2679–2693, 2009.

[10] J.C Bezdek, *Pattern Recognition with fuzzy objective function algorithm*, Plenum Press, 1981.

[11] H. Frigui and R. Krishnapuram, "A robust competitive clustering algorithm with applications in computer vision," *IEEE Trans. on Pattern Analysis and Machine Intelligence*, vol. 21, no. 5, pp. 450–465, May 1999.

[12] M. Berman, H. Kiiveri, R. Lagerstrom, A. Ernst, R. Donne, and J. F. Huntington, "ICE: A statistical approach to identifying endmembers in hyperspectral images," *IEEE Trans. on Geoscience and Remote Sensing*, vol. 42, pp. 2085–2095, Oct. 2004.

[13] A. Zare and P. Gader, "Sparsity promoting iterated constrained endmember detection for hyperspectral imagery," *IEEE Geoscience and Remote Sensing Letters*, vol. 4, no. 3, pp. 446–450, July 2007.

[14] S. Krinidis and V. Chatzis, "A robust fuzzy local information c-means clustering algorithm," *IEEE Transactions on Image Processing*, 2010, In Press.